NANO LETTERS

Letter

pubs.acs.org/NanoLett

Ultrastrong Optical Binding of Metallic Nanoparticles

Vassili Demergis and Ernst-Ludwig Florin*

Center for Nonlinear Dynamics and Department of Physics, The University of Texas at Austin, 1 University Station, C1600 Austin, Texas 78712-0264, United States

Supporting Information

ABSTRACT: We demonstrate nanometer precision manipulation of multiple nanoparticles at room temperature. This is achieved using the optical binding force, which has been assumed to be weak compared to the optical gradient and scattering forces. We show that trapping by the optical binding force can be over 20 times stronger than by the gradient force and leads to ultrastable, rigid configurations of multiple nanoparticles free in solution − a realization of "optical matter." In addition, we demonstrate a novel trapping scheme where even smaller nanoparticles are trapped between larger "anchor" particles. Optical binding opens the door for the observation of collective phenomena of nanoparticles and the design of new materials and devices made from optical matter.

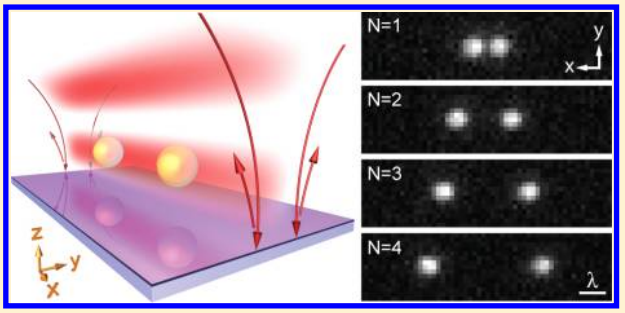

KEYWORDS: *Optical binding, optical trapping, optical molecules, optical matter, nanostructures, photonics, nanoparticle assembly*

Since the first demonstration of optical trapping using the optical scattering and gradient forces,[1,2] optical manipulation of matter has found wide application not only in fundamental physics but also in fields as diverse as physical chemistry, cell biology, and nanotechnology.[1−9] At first, micrometer-sized objects were trapped such as bacteria, while smaller objects required increased laser intensity in order for optical forces to overcome thermal forces. Stable trapping of single atoms was eventually achieved only when advanced techniques for cooling atoms to near absolute zero were employed, thus minimizing thermal motion. Yet the most groundbreaking results came when multiple atoms were trapped simultaneously, which is essential for the observation of macroscopic quantum phenomena such as the Bose−Einstein condensate[10] and the atom laser.[11]

Unfortunately cooling is not an option for studying dynamics that occur at room temperature or in aqueous solution, and an efficient way to manipulate and study large numbers of nanoparticles with high precision has yet to be developed. Multiple particles can be manipulated by using, for example, holographic or scanning optical tweezers.[3−5,8] However, such techniques require the laser intensity to be widely distributed, and the specially shaped light fields are easily perturbed by the introduction of additional optics resulting in reduced trapping strength and precision.[5] Therefore particles must typically be micrometers in size in order for optical forces to overcome thermal forces, and precise control is still lost due to thermal motion. Increased laser intensity can be used to generate stronger forces, finer control, or for trapping smaller objects. However, the maximal intensity is limited by heating and radiation damage to the sample, such as with biological material.[5,12,13] Focus has been mainly placed on strengthening the optical gradient force while weakening the destabilizing optical scattering force, such as with variations on optical tweezer geometry,[3,6−9,12,14,15] yet this path has so far produced only limited improvement.

In this work, we demonstrate that a third optical force, the optical binding (OB) force,[16−33] can be used as a powerful tool for high-precision, simultaneous control of multiple nanoparticles without the need for specially shaped light fields. OB was originally assumed to be significant only in intense optical fields and weaker than the gradient force.[17,22] However, we show that trapping by OB can be 20 times stronger and more efficient than by the gradient force in even the best optimized optical tweezers. This leads to ultrastrong interactions between multiple nanoparticles that freeze their relative position within tens of nanometers, a realization of "optical matter."[17] We characterize in detail the formed "optical molecules," which resemble traditional molecules where nanoparticles substitute for the atoms, and optical binding forces substitute for the chemical bonds, as model systems for larger scale optical matter.

The OB force was first observed in 1989,[16] only a few years after the optical gradient force trap was developed.[2] It was observed that when two or more particles are present in an optical field, their motion becomes coupled due to interactions between the induced electric currents and scattered fields. The most distinct indicator of this coupling is the seemingly quantized position states which the particles like to rest, an effect of the OB force's periodicity with separation distance (R) between particles. More intriguing is the length scale at which the interactions occur. The OB interaction energy decays only

Received: August 14, 2012
Revised: September 29, 2012
Published: October 4, 2012

ACS Publications © 2012 American Chemical Society

as $1/R$ in the far-field compared to more typical dipole−dipole interactions that decay much more rapidly ($E_{\text{Coulomb}} \propto 1/R^3$, $E_{\text{Van der Waals}} \propto 1/R^6$).[16,17,23,27] This potentially allows for the formation of so-called "optical matter," contactless but rigid particle formations held together by OB forces,[17,22] as well as for new optical trapping and sorting systems.[24,26]

Optical binding between a pair of particles can be described by classical electrodynamics, and most simply for Rayleigh particles ($ka \ll 1$, where $k = 2\pi/\lambda$ is the wavenumber of excitation light in the medium and a is the particle radius). However, until now, a detailed quantitative experiment dealing with nanoparticle binding has not been reported.[31] By utilizing a standing wave optical line trap[15] (SWOLT), it is possible to stably confine nanoparticles to essentially one-dimension due to the shape of the optical intensity field. Individual particles are free to diffuse over many micrometers along the long axis of the trap (x-axis) while confined to only tens of nanometers along the other two axes.[15] When two or more particles are confined in the same SWOLT, their thermal motion becomes further restricted by OB forces (see Figure 1). However, this restriction is placed on their relative positions, not absolute positions, resulting in coupled motion. The OB energy landscape[30] between two particles is known to be a series of roughly equally spaced energy minima at particle−particle separations of $R_N \approx \lambda N$ where $N = \{1,2,3...\}$. Therefore, it has been observed that particle pairs transiently "hop" between these minima due to their combined thermal energy being larger than the OB energy barriers.[16,17,21] In the case where OB forces dominate over thermal forces, we would expect that the particles maintain a constant separation distance determined by the nearest OB energy minimum when the particles become first illuminated. This effect has previously been observed only for very large particles ($ka > 1$) along the axis of light propagation (termed longitudinal OB)[20,25,29] or for particles whose thermal motion is dampened from contact with a surface[16,17,33] as in total internal reflection methods.

In our experiments, we observe dramatic binding strength between particles with size closer to the Rayleigh regime ($ka \approx 0.8$) and in a direction perpendicular to the direction of light propagation (termed lateral or transverse OB). This lateral OB configuration allows us to precisely image the particles using the same microscope optics which focus the laser and also study the polarization dependence of the OB, which is not possible in longitudinal OB experiments. Using the SWOLT, we confine 200 nm diameter gold particles in water ($n_m = 1.33$) using a $\lambda_0 = n_m\lambda = 1064$ nm wavelength laser at roughly $\lambda/4 = 200$ nm above the reflecting coverslip surface (Figure 1). At this distance above the surface, about two particle radii, near-surface effects to OB forces have been shown to be minimal,[19,31,34] and more importantly there is no contact between particle and surface due to the strong axial intensity gradients.[14,15]

Using only modest laser power ($P \approx 70$ mW, measured in the focal plane), particles maintain a constant separation distance on the order of micrometers while only deviating from that precise distance by a few tens of nanometers (Figure 2b). This behavior is conceptually similar to two particles joined together by a spring of rest length R_N and spring constant κ_N (Figure 1c). Figure 2a shows dark-field images (Supporting Information Videos 1−4) of optically bound particles in the SWOLT in different binding positions. We stress that these binding positions are stable for many hours despite thermal fluctuations at room temperature. We prompt particles to hop to different positions either by briefly decreasing laser power

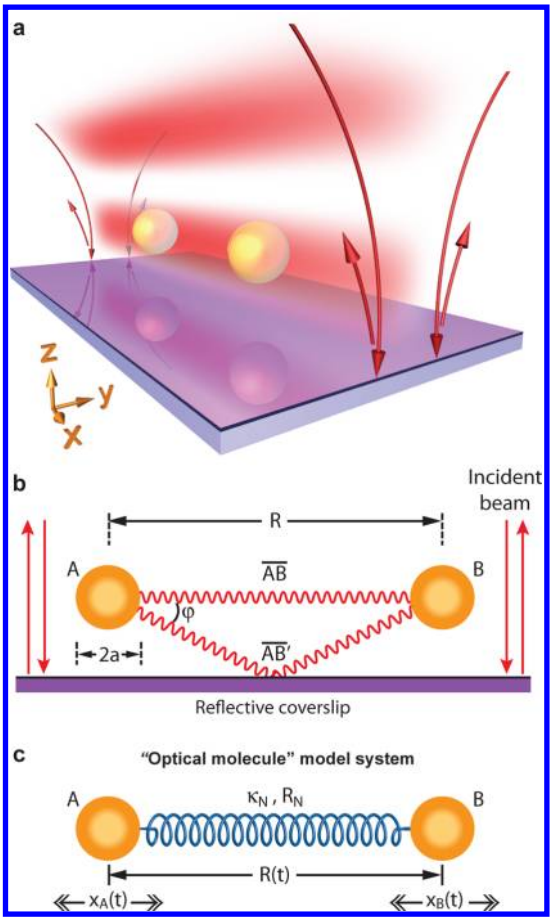

Figure 1. Schematic of optical binding in a standing wave optical line trap. (a) A 3D schematic representation of two gold nanoparticles trapped and aligned in the first intensity maximum of the standing wave. The intensity gradients along the y- and z-axes are much greater than along the x-axis, essentially restricting motion to 1D along the x-axis.[15] (b) Diagram showing the interaction of two particles of radius a via scattered light waves (wavy lines). The optical binding force in this system is due to the direct scattered wave from particle A to particle B (path length $\overline{AB}$), as well as the portion of the scattered wave reflected off the dichroic coverslip surface ($\overline{AB}'$). A similar treatment of OB near a reflective surface has been described in ref 32. (c) Ultrastable optically bound particle pairs can be modeled as two particles attached by a spring of rest length R_N and spring constant κ_N. Each particle contains thermal energy of k_BT that causes fluctuations in the measured center-to-center distance $R(t)$ about R_N.

(below 10%), thus lowering the OB energy barrier, or by releasing and retrapping the particles (turning the laser off then on). For each binding position, we obtain a video of the particle motion for quantitative tracking and analysis. Figure 2b shows histograms of the measured separation distance R between the particles. Eight individual data sets are shown corresponding to the eight peaks in Figure 2b.

The histograms in Figure 2b show particle separation distances near multiples of the laser wavelength $R_N \approx \lambda N$. However, we can also see deviation from this simple approximation. Notably, we see distinct shifts in the histogram centers when the polarization is rotated for a given binding position N. This shift is on the order of tens of nanometers, and becomes smaller as R increases. This is in agreement with theoretical predictions.[18,19,31] Figure 2c shows measurements of the average separation distance R_N compared with theoretical predictions (Supporting Information Section 1) of the stable

dx.doi.org/10.1021/nl303035p | Nano Lett. 2012, 12, 5756−5760

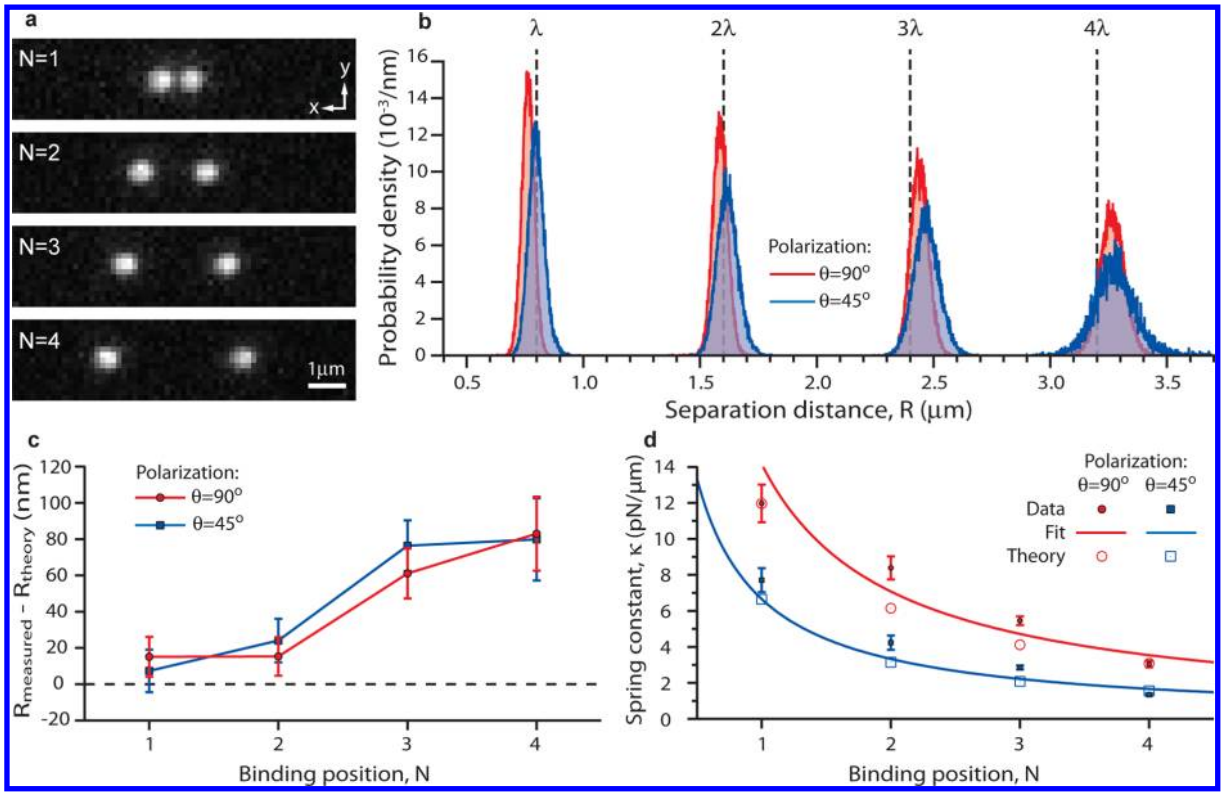

Figure 2. Measurement of the binding positions and binding forces between two gold nanoparticles. (a) Dark-field images of 200 nm diameter gold particles exhibiting optical binding while confined to 1D motion along the *x*-axis in the SWOLT. These optically bound particles diffuse easily along the *x*-axis, but maintain a precise separation distance *R* over long time scales (typically hours) with only slight fluctuations. Only by releasing and retrapping the particles can they quickly fall into different binding configurations. The closest (most stable) four binding positions are shown. Videos were recorded at 70 fps with 10 μs exposure time, and particle positions were obtained by video tracking. Scale bar: 1 μm. (b) Histograms of the particle separation distance were constructed from the data of particle motion. Shown are individual histograms from eight different data traces using the same pair of gold nanoparticles but in four different binding positions and for two different polarization angles of the incident laser relative to the binding axis (*x*-axis). Each histogram is composed of 30 000 data points (≈7 min video) except for the histogram of $N = 4$ with $\theta = 45°$ that consists of only 10 000 data points due to the lower stability. Bin width = 1 nm. The average binding distance is notably different than simple multiples of the wavelength and shifts when the polarization of the incident light is rotated. The widths of the histograms, while only tens of nanometers wide, can be seen to increase with greater separation distance, indicating weaker binding as the scattered field decreases in strength with distance. (c) The measured average separation obtained from the histograms is compared with theoretical predictions (Supporting Information Section 1). The particles sit further apart than theoretical predictions, but are pulled closer together at shorter separations due to path length differences between the direct and reflected scattered waves. The error bars include consideration of the error in least-squares fitting, particle tracking algorithm, camera field of view calibration, long time scale drift and the standard error. (d) The measured optical binding spring constant is compared to theoretical predictions and a β/N fit to the data where β is the only fitting parameter. The interparticle spring constant κ is calculated directly from the widths of the histograms. The strength of the binding is seen to decrease with distance and with rotation of the polarization of the incident beam as predicted by the theory. The error bars include consideration of the error in least-squares fitting, particle tracking algorithm, camera field of view calibration, room temperature fluctuations, and long time scale drift.

positions and illustrates the precision of our measurements. While the difference between measurement and theory is relatively small (<100 nm = $\lambda/8$), we can see that the particles tend to be separated by greater distances than predicted, especially at larger average separations. This difference arises because the particles are not point objects and from the inclusion of the reflective surface (for further discussion, see Supporting Information Section 2).

The widths of the histograms in Figure 2b report on the precision and strength of the OB forces. We can see that as the separation distance increases, the widths of the histograms also increase which indicates weaker binding. This is due to the magnitude of the scattered field decaying with distance from the scatterer. We also see weaker binding when the polarization angle θ decreases because the scattered field is weaker and decays much more quickly along the axis of the induced dipole moment. These results are in agreement with theory.[18,19,22,31]

We quantify the OB forces by considering the model in Figure 1c. The thermal fluctuations of the particle−particle separation distance about the average binding position R_N is related to the spring constant κ_N by Maxwell−Boltzmann statistics as $\kappa_N = 4k_BT/\sigma_N^2$ (Supporting Information Sections 3 and 4) where k_B is Boltzmann's constant, T is the sample temperature and σ_N is the width of the Gaussian probability distribution (Figure 2b). While heating of gold nanoparticles during optical trapping has been reported and characterized, for our system we estimate no significant heating of the particles because of the low local laser intensity (Supporting Information Section 5). Therefore we can assume the temperature of the sample is approximately room temperature. Figure 2d compares the measured values of κ_N with calculated values (Supporting Information Section 6), and we see general agreement. The OB spring constant decreases as roughly $1/N$ as expected (Supporting Information Section 7).

dx.doi.org/10.1021/nl303035p | Nano Lett. 2012, 12, 5756−5760

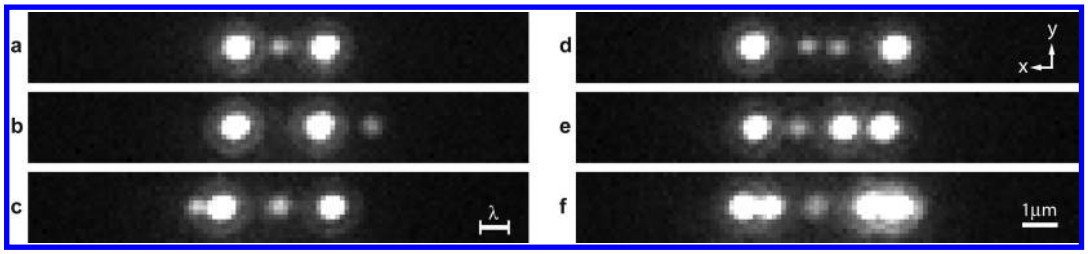

Figure 3. Assisted trapping of nanoparticles using optical binding forces. A mixture of 200 and 100 nm diameter gold particles were trapped and aligned in the SWOLT. For the trapping laser power used (70 mW in the focal plane), the smaller particles on their own exhibit large thermal fluctuations along the *x*-axis. However, by using the larger particles as an anchor, the smaller particles become effectively confined due to the strong optical binding forces. Shown are a few sample configurations of small particles trapped with help from the larger anchor particles. See also Supporting Information Section 9. Scale bar: λ = 800 nm.

The strength of the OB force and its decay with distance is an important consideration if one intends to design an OB trap,[24,26] but equally important is the laser intensity used to generate these traps. Trapping smaller objects generally requires larger laser intensities which may eventually heat or damage the objects.[5,12,13] Therefore we define the trapping efficiency as $\xi \equiv \kappa/I$ where I is the local laser intensity at the trapped object. We can compare the trapping efficiency of the strongest OB forces measured here (at N = 1, θ = 90°) with that of the best optimized optical tweezers (OT), whose trapping efficiency has been characterized in detail for similar sized gold particles using the same laser wavelength.[35] We find $\xi_{OB}/\xi_{OT} \approx 22$ (Supporting Information Section 8). This ultraefficient OB force has potential to be used in new optical trapping designs where sensitivity to laser intensity is a concern. One possible design uses the strong OB forces generated between large particles to assist trapping of smaller particles. The dark-field images in Figure 3 show configurations of large (200 nm diameter) and small (100 nm diameter) gold particles in the SWOLT. The smaller particles individually fluctuate long distances in the SWOLT, but in the presence of larger "anchor" particles, they are effectively contained by OB forces (Supporting Information Videos 5 and 6).

In conclusion, we have shown that the OB force is a unique and powerful tool for manipulation of multiple nanoparticles. This ultrastrong, long-range interaction can be used to create complex rigid nanostructures[22] with very high precision. With reasonably increased laser intensity and by using a laser wavelength near the plasmon resonance of the particles, precision of only a few nanometers or better should be achievable. Even particles 45 nm in diameter or smaller should stably bind although with less precision (Supporting Information Section 10). We also expect that optical matter should become more stable as more particles are added, and as we have indicated by our assisted trapping design, binding of smaller nanoparticles to form larger optical molecules should result in stable trapping of the object as a whole whereas the individual components may normally be difficult to trap. There is vast potential for commercial application of optical matter. For example, metal particles or nanowires may be arranged precisely in 3D using OB then frozen in place within light-activated resin,[4] thereby keeping the arrangement in a material for use in new electronics such as novel photovoltaics[36,37] or high-precision plasmonic nanodevices.[38,39] Seeds or templates may be made for generating crystal structures or even biological tissue.[8,31] New designs for nanomachines based on OB forces are now possible that can switch conformations or functions when illuminated by different wavelengths. When sensitivity to laser intensity is a concern, such as with biological experiments,[12] OB provides the possibility for ultralow power optical manipulation thereby extending the realm of potential medical research.

■ ASSOCIATED CONTENT

Supporting Information

Additional details of the theoretical calculations and data analysis; videos of optically bound particles in a SWOLT. This material is available free of charge via the Internet at http://pubs.acs.org.

■ AUTHOR INFORMATION

Corresponding Author

*Phone: (512) 471-6441. Fax: (512) 471-1558. E-mail: florin@chaos.utexas.edu.

Notes

The authors declare no competing financial interest.

■ ACKNOWLEDGMENTS

The authors would like to thank Andrea Keidel and Kathleen Hinko for helpful discussions.

■ ABBREVIATIONS

OB, optical binding; SWOLT, standing wave optical line trap; OT, optical tweezers

■ REFERENCES

(1) Ashkin, A. Acceleration and trapping of particles by radiation pressure. *Phys. Rev. Lett.* **1970**, *24*, 156−159.

(2) Ashkin, A.; Dziedzic, J. M.; Bjorkholm, J. E.; Chu, S. Observation of a single-beam gradient force optical trap for dielectric particles. *Opt. Lett.* **1986**, *11*, 288−290.

(3) Grier, D. G. A revolution in optical manipulation. *Nature* **2003**, *424*, 810−816.

(4) Jordan, P.; Leach, J.; Padgett, M.; Blackburn, P.; Isaacs, N.; Goksor, M.; Hanstorp, D.; Wright, A.; Girkin, J.; Cooper, J. Creating permanent 3D arrangements of isolated cells using holographic optical tweezers. *Lab Chip* **2005**, *5*, 1224−1228.

(5) Neuman, K. C.; Nagy, A. Single-molecule force spectroscopy: optical tweezers, magnetic tweezers and atomic force microscopy. *Nat. Methods* **2008**, *5*, 491−505.

(6) Jonas, A.; Zemanek, P. Light at work: The use of optical forces for particle manipulation, sorting, and analysis. *Electrophoresis* **2008**, *29*, 4813−4851.

(7) Dienerowitz, M.; Mazilu, M.; Dholakia, K. Optical manipulation of nanoparticles: a review. *J. Nanophotonics* **2008**, *2*, 021875.

(8) Cizmar, T.; Davila Romero, L. C.; Dholakia, K.; Andrews, D. L. Multiple optical trapping and binding: new routes to self-assembly. *J. Phys. B: At. Mol. Phys.* **2010**, *43*, 102001.

(9) Fazal, F. M.; Block, S. M. Optical tweezers study life under tension. *Nat. Photonics* **2011**, *5*, 318−321.
(10) Anderson, M. H.; Ensher, J. R.; Matthews, M. R.; Wieman, C. E.; Cornell, E. A. Observation of Bose-Einstein condensation in a dilute atomic vapor. *Science* **1995**, *269*, 198−201.
(11) Inouye, S.; Pfau, T.; Gupta, S.; Chikkatur, A. P.; Gorlitz, A.; Pritchard, D. E.; Ketterle, W. Phase-coherent amplification of atomic matter waves. *Nature* **1999**, *402*, 641−644.
(12) Neuman, K. C.; Chadd, E. H.; Liou, G. F.; Bergman, K.; Block, S. M. Characterization of photodamage to Escherichia coli in optical traps. *Biophys. J.* **1999**, *77*, 2856−2863.
(13) Jannasch, A.; Demirors, A. F.; van Oostrum, P. D. J.; van Blaaderen, A.; Schaffer, E. Nanonewton optical force trap employing anti-reflection coated, high-refractive-index titania microspheres. *Nat. Photonics* **2012**, *6*, 469−473.
(14) Zemanek, P.; Jonas, A.; Sramek, L.; Liska, M. Optical trapping of Rayleigh particles using a Gaussian standing wave. *Opt. Commun.* **1998**, *151*, 273−285.
(15) Demergis, V.; Florin, E.-L. High precision and continuous optical transport using a standing wave optical line trap. *Opt. Express* **2011**, *19*, 20833−20848.
(16) Burns, M. M.; Fournier, J.-M.; Golovchenko, J. A. Optical binding. *Phys. Rev. Lett.* **1989**, *63*, 1233−1236.
(17) Burns, M. M.; Fournier, J.-M.; Golovchenko, J. A. Optical matter: crystallization and binding in intense optical fields. *Science* **1990**, *249*, 749−754.
(18) Depasse, F.; Vigoureux, J.-M. Optical binding force between two Rayleigh particles. *J. Phys. D: Appl. Phys.* **1994**, *27*, 914−919.
(19) Nieto-Vesperinas, M.; Chaumet, P. C. Optical binding of particles with or without the presence of a flat dielectric surface. *Phys. Rev. B* **2001**, *64*, 035422.
(20) Tatarkova, S. A.; Carruthers, A. E.; Dholakia, K. One-dimensional optically bound arrays of microscopic particles. *Phys. Rev. Lett.* **2002**, *89*, 283901.
(21) Mohanty, S. K.; Andrews, J. T.; Gupta, P. K. Optical binding between dielectric particles. *Opt. Express* **2004**, *12*, 2749−2756.
(22) Ng, J.; Lin, Z. F.; Chan, C. T.; Sheng, P. Photonic clusters formed by dielectric microspheres: numerical simulations. *Phys. Rev. B* **2005**, *72*, 085130.
(23) Bradshaw, D. S.; Andrews, D. L. Optically induced forces and torques: Interactions between nanoparticles in a laser beam. *Phys. Rev. A* **2005**, *72*, 033816.
(24) Grzegorczyk, T. M.; Kemp, B. A.; Kong, J. A. Stable optical trapping based on optical binding forces. *Phys. Rev. Lett.* **2006**, *96*, 113903.
(25) Guillon, M.; Moine, O.; Stout, B. Longitudinal optical binding of high contrast microdroplets in air. *Phys. Rev. Lett.* **2006**, *96*, 143902.
(26) Grzegorczyk, T. M.; Kemp, B. A.; Kong, J. A. Passive guiding and sorting of small particles with optical binding forces. *Opt. Lett.* **2006**, *31*, 3378−3380.
(27) Salam, A. Two alternative derivations of the static contribution to the radiation-induced intermolecular energy shift. *Phys. Rev. A* **2007**, *76*, 063402.
(28) Dienerowitz, M.; Mazilu, M.; Reece, P. J.; Krauss, T. F.; Dholakia, K. Optical vortex trap for resonant confinement of metal nanoparticles. *Opt. Express* **2008**, *16*, 4991−4999.
(29) Karasek, V.; Cizmar, T.; Brzobohaty, O.; Zemanek, P.; Garces-Chavez, V.; Dholakia, K. Long-range one-dimensional longitudinal optical binding. *Phys. Rev. Lett.* **2008**, *101*, 143601.
(30) Rodriguez, J.; Davila Romero, L. C.; Andrews, D. L. Optical binding in nanoparticle assembly: Potential energy landscapes. *Phys. Rev. A* **2008**, *78*, 043805.
(31) Dholakia, K.; Zemanek, P. Colloquium: Gripped by light: Optical binding. *Rev. Mod. Phys.* **2010**, *82*, 1767−1791.
(32) Brzobohaty, O.; Cizmar, T.; Karasek, V.; Siler, M.; Dholakia, K.; Zemanek, P. Experimental and theoretical determination of optical binding forces. *Opt. Express* **2010**, *18*, 25389−25401.
(33) Summers, M. D.; Dear, R. D.; Taylor, J. M.; Ritchie, G. A. D. Directed assembly of optically bound matter. *Opt. Express* **2012**, *20*, 1001−1012.
(34) Chaumet, P. C.; Nieto-Vesperinas, M. Coupled dipole method determination of the electromagnetic force on a particle over a flat dielectric substrate. *Phys. Rev. B* **2000**, *61*, 14119−14127.
(35) Hajizadeh, F.; Reihani, S. N. S. Optimized optical trapping of gold nanoparticles. *Opt. Express* **2010**, *18*, 551−559.
(36) Nishijima, Y.; Ueno, K.; Yokota, Y.; Murakoshi, K.; Misawa, H. Plasmon-assisted photocurrent generation from visible to near-infrared wavelength using a Au-nanorods/TiO2 electrode. *J. Phys. Chem. Lett.* **2010**, *1*, 2031−2036.
(37) Nishijima, T.; Rosa, L.; Juodkazis, S. Surface plasmon resonances in periodic and random patterns of gold nano-disks for broadband light harvesting. *Opt. Express* **2012**, *20*, 11466−11476.
(38) Barnes, W. L.; Dereux, A.; Ebbesen, T. W. Surface plasmon subwavelength optics. *Nature* **2003**, *424*, 824−830.
(39) Gramotnev, D. K.; Bozhevolnyi, S. I. Plasmonics beyond the diffraction limit. *Nat. Photonics* **2010**, *4*, 83−91.